This article was downloaded by: [Chongqing University]
On: 14 February 2014, At: 13:34
Publisher: Taylor & Francis
Informa Ltd Registered in England and Wales Registered Number: 1072954 Registered office: Mortimer House, 37-41 Mortimer Street, London W1T 3JH, UK

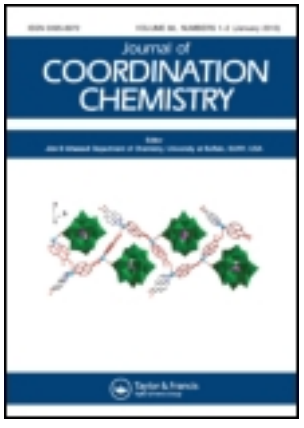

Journal of Coordination Chemistry
Publication details, including instructions for authors and subscription information:
http://www.tandfonline.com/loi/gcoo20

Coordination behavior of chromone Schiff bases towards the $[Re^{V}O]^{3+}$ and $[Re^{I}(CO)_3]^{+}$ cores

Irvin Noel Booysen[a], Muhammed Bilaal Ismail[a] & Matthew Piers Akerman[a]
[a] School of Chemistry and Physics, University of Kwazulu-Natal, Scottsville, Pietermaritzburg, South Africa
Published online: 10 Dec 2013.

To cite this article: Irvin Noel Booysen, Muhammed Bilaal Ismail & Matthew Piers Akerman (2013) Coordination behavior of chromone Schiff bases towards the $[Re^{V}O]^{3+}$ and $[Re^{I}(CO)_3]^{+}$ cores, Journal of Coordination Chemistry, 66:24, 4371-4386, DOI: 10.1080/00958972.2013.867028

To link to this article: http://dx.doi.org/10.1080/00958972.2013.867028

PLEASE SCROLL DOWN FOR ARTICLE

Taylor & Francis makes every effort to ensure the accuracy of all the information (the "Content") contained in the publications on our platform. However, Taylor & Francis, our agents, and our licensors make no representations or warranties whatsoever as to the accuracy, completeness, or suitability for any purpose of the Content. Any opinions and views expressed in this publication are the opinions and views of the authors, and are not the views of or endorsed by Taylor & Francis. The accuracy of the Content should not be relied upon and should be independently verified with primary sources of information. Taylor and Francis shall not be liable for any losses, actions, claims, proceedings, demands, costs, expenses, damages, and other liabilities whatsoever or howsoever caused arising directly or indirectly in connection with, in relation to or arising out of the use of the Content.

This article may be used for research, teaching, and private study purposes. Any substantial or systematic reproduction, redistribution, reselling, loan, sub-licensing, systematic supply, or distribution in any form to anyone is expressly forbidden. Terms & Conditions of access and use can be found at http://www.tandfonline.com/page/terms-and-conditions

Journal of Coordination Chemistry, 2013
Vol. 66, No. 24, 4371–4386, http://dx.doi.org/10.1080/00958972.2013.867028

Taylor & Francis
Taylor & Francis Group

Coordination behavior of chromone Schiff bases towards the $[Re^{V}O]^{3+}$ and $[Re^{I}(CO)_3]^{+}$ cores

IRVIN NOEL BOOYSEN*, MUHAMMED BILAAL ISMAIL and MATTHEW PIERS AKERMAN*

School of Chemistry and Physics, University of Kwazulu-Natal, Scottsville, Pietermaritzburg, South Africa

(*Received 22 July 2013; accepted 7 November 2013*)

Herein, we describe the coordination behavior of chromone Schiff bases towards $[Re^{V}O]^{3+}$ and $[Re^{I}(CO)_3]^{+}$. The reaction between 2-(2-thiolphenyliminomethyl)-4*H*-chromen-4-one (Htch) and $[Re(CO)_5Cl]$ led to *fac*-$[Re(CO)_3(bsch)Cl]$ (**1**) (bsch = 2-benzothiazole-4*H*-chromen-4-one). The square pyramidal [ReO(Hns)] (**2**) {H_2ns = *bis*-[(2-phenylthiolate)iminomethyl]-methyl-1-(2-hydroxyphenyl)prop-2-en-1-one} and octahedral $[ReO(OCH_3)(PPh_3)(Huch)]$ (**3**) complexes were isolated from reactions of *trans*-$[Re^{V}OBr_3(PPh_3)_2]$ with Htch and H_3uch [(5*Z*)-5-((4-hydroxy-2-methoxy-2*H*-chromen-3-*yl*)methyleneamino)-6-amino-1,3-dimethylpyrimidine-2,4(*1H*, *3H*)-dione], respectively. The chromone Schiff bases and their metal complexes were fully characterized *via* NMR-, IR- and UV–Vis spectroscopy, single crystal XRD analysis and conductivity measurements. In addition, DFT studies were conducted to compare selected optimized and experimental parameters of the complexes.

Keywords: Rhenium (I/V); Schiff bases; Chromone; Crystal structure; DFT studies

Downloaded by [Chongqing University] at 13:34 14 February 2014

1. Introduction

The coordination chemistry of rhenium has been widely explored since the discovery of a target-specific rhenium radiopharmaceutical depends on its stability, geometry and the attachment of a biologically active molecule (BAM) to the $^{186/188}$Re radionuclide [1, 2]. Schiff bases can be readily derived from BAMs and this ligand system has shown to be excellent chelators to rhenium, thereby stabilizing the metal in both the low and high oxidation states [3, 4]. This stabilization is largely accounted to their diverse donor atoms, chelation and multidenticity upon coordination [5, 6]. Subsequently, these attributes of Schiff bases afford rhenium complexes with different structural features [8]. An example is the rhenium(I) complex, *fac*-$[Re(msh)(py)(CO)_3]$ [Hmsh = 2-[(2-indol-3-*yl*-ethyl)iminomethyl]-5-methylphenol], in which a stable 6-membered chelate ring formed through the deprotonated phenolic oxygen and imino nitrogen, while the indole moiety remained uncoordinated [11].

Beside the influential coordination capability of Schiff bases, these organic compounds have shown to exhibit a wide array of biological activity [12–14]. In particular, Schiff bases derived from 3-formyl chromone and their corresponding transition metal complexes have

*Corresponding authors. Email: Booyseni@ukzn.ac.za (IN Booysen); Akermanm@ukzn.ac.za (MP Akerman)

© 2013 Taylor & Francis

displayed optimal anti-thymidine phosphorylase inhibitory-, antibacterial-, antioxidant- and antifungal activity as well DNA binding capabilities. In addition, the chromone Schiff base, 7-methoxychromone-3-carbaldehyde-(3,4-dimethyl)-pyrrole hydrazone has shown selective chemosensing capability for the toxic Al^{3+} species in the presence of other metal cations [15].

From a coordination chemistry perspective, chromone Schiff bases typically form coordination bonds through the imino nitrogen and the keto/enol oxygen as well as donor atoms on neighboring (with respect to the Schiff base group) aliphatic or aromatic moieties [16–21]. A typical example is the neutral tridentate chelator 6-hydroxychromone-3-carbaldehydethiosemicarbazone, which coordinates to the Ni^{2+} metal atom through the classical $N_{imino},O_{ketonic}$ donor set as well as the thiocarbonyl sulfur atom of the thiosemicarbazone moiety [22].

In this account, we explored the coordination behavior of Schiff bases incorporating a chromone moiety towards the *fac*-$[Re^{I}(CO)_3]^+$ and $[Re^{V}O]^{3+}$ cores. Three rhenium compounds, *fac*-$[Re^{I}(CO)_3$(bsch)Cl] (**1**) (bsch = 2-benzothiazole-4*H*-chromen-4-one), $[Re^{V}O$(Hns)] (**2**) {H_2ns=*bis*-[(2-phenylthiolate)iminomethyl]-methyl-1-(2-hydroxyphenyl)prop-2-en-1-one} and $[Re^{V}O(OCH_3)(PPh_3)$(Huch)] (**3**) [Huch = (5*Z*)-5-((4-hydroxy-2-methoxy-2*H*-chromen-3-*yl*) methyleneamino)-6-amino-1,3-dimethylpyrimidine-2,4-(*1H*,*3H*)-dione], were isolated. The 2-(2-thiolphenyliminomethyl)-4*H*-chromen-4-one (Htch) Schiff base was reacted with $[Re^{I}(CO)_5Cl]$ and *trans*-$[Re^{V}OBr_3(PPh_3)_2]$ to form **1** and **2**, respectively. The ligand cyclized to afford the bidentate heterocyclic chelator, bsch (in **1**), and transformed to form a N_2S_2 tetradentate chelator (in **2**). In **3**, free H_3uch did not transform or cyclize but rather coordinated as the Huch dianionic tridentate chelator.

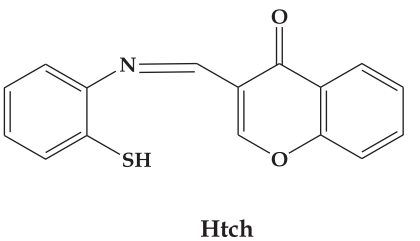

Htch

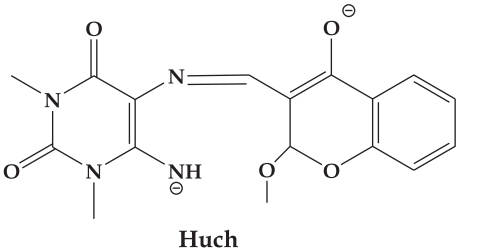

Huch

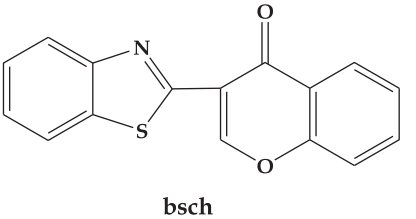

bsch

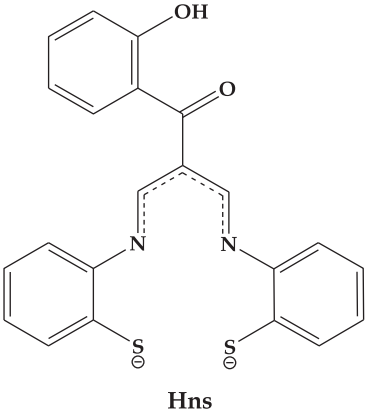

Hns

Downloaded by [Chongqing University] at 13:34 14 February 2014

Downloaded by [Chongqing University] at 13:34 14 February 2014

2. Experimental

2.1. *Materials and methods*

Pentacarbonylrhenium(I)chloride, ammonium perrhenate, 4-oxo-4*H*-chromene-3-carbaldehyde, 2-aminothiophenol and 5,6-diamino-1,3-dimethyl uracil were obtained from Sigma Aldrich. All solvents were obtained from Merck SA. The rhenium(V) metal precursor, *trans*-[ReOBr$_3$(PPh$_3$)$_2$], was synthesized as previously reported [23]. The chemicals were used without any further purification. Ultrapure water was produced from an Elga Purelab Ultra system.

The infrared spectra were recorded on a Perkin–Elmer Spectrum 100 from 4000–650 cm^{-1}. ^{1}H NMR spectra were obtained using a Bruker Avance 400 MHz spectrometer. All NMR spectra were recorded in DMSO-d$_6$ except for **1**, which was recorded in deuterated dichloromethane (CD_2Cl_2). UV–Vis spectra were recorded using a Perkin–Elmer Lambda 25. Melting points were determined using a Stuart SMP3 melting point apparatus. The conductivity measurements were determined at 295 K on a Radiometer R21M127 CDM 230 conductivity and pH meter.

2.2. *3-{(Z)-[(2-Sulfanylphenyl)imino]methyl}-4H-chromen-4-one (Htch)*

2-Aminobenzenethiol (0.154 cm^3, 1.44 mM) and 3-formylchromone (0.250 g, 1.44 mM) were refluxed in 25 cm^3 of MeOH. After 3 h, the solution was reduced to 10 cm^3 and the yellow precipitate was filtered. The precipitate was washed with cold MeOH and petroleum ether. Yield = 63%. M.P. 224.4 – 228.6 °C; IR (ν_{max}/cm^{-1}): *ν*(S–H) 3309, *ν*(C=O) 1618, *ν*(C=N) 1595, *ν*(C=C) 1456; ^{1}H NMR (295K/ppm): (figure S1, see online supplemental material at http://dx.doi.org/10.1080/00958972.2013.867028) 8.24 (s, 1H, *H1*), 8.09 (d, 1H, *H8*), 7.83 (t, 1H, *H9*), 7.68 (d, 1H, *H5*), 7.51 (t, 1H, *H3*), 7.01 (d, 1H, *H2*), 6.89 (t, 1H, *H10*), 6.68-6.71 (m, 2H, S*H*, *H6*), 6.61 (t, 1H, *H4*), 6.40 (d, 1H, *H11*). UV–Vis (DMF, λ_{max} (ε, M^{-1}cm^{-1})): 296 nm (9056), 313 nm (11513).

2.3. *(5Z)-5-((4-Hydroxy-2-methoxy-2H-chromen-3-yl)methyleneamino)-6-amino-1,3-dimethylpyrimidine-2,4(1H, 3H)-dione (H_3uch)*

1,3-Dimethyl-5,6-diamino uracil (0.244 g, 1.44 mM) and 3-formylchromone (0.250 g, 1.44 mM) were dissolved in MeOH (35 cm^3) and stirred for 3 h under reflux. The fluffy yellow precipitate was filtered and washed with cold methanol and petroleum ether. Yield = 66%. M.P. 282.7 – 284.9 °C; IR (ν_{max}/cm^{-1}): *ν*(O–H) 3434, *ν*(N–H) 3309, *ν*(C=O) 1683, *ν*(C=N) 1613, *ν*(C=C) 1583; ^{1}H NMR (295K/ppm): (see figure S2) 9.78 (s, 1H, *H1*), 9.28 (s, 1H, *H6*), 8.13 (d, 1H, *H5*), 7.82 (t, 1H, *H4*), 7.70 (d, 1H, *H2*), 7.52 (t, 1H, *H3*), 7.41 (br, s, 2H, NH_2), 6.89 (s, 2H, NH_2), 3.87 (s, 3H, C(8)H_3), 3.76 (s, 3H, C(7)H_3), 3.31 (br, s, 1H, O*H*), 3.18 (s, 3H, OC(10)H_3). UV–Vis (DMF, λ_{max} (ε, M^{-1}cm^{-1})): 294 nm (3004), 358 nm (2632).

2.4. *fac-[Re(CO)$_3$(bsch)Cl] (1)*

Htch (0.069 g, 0.246 mM) was added to [Re(CO)$_5$Cl] (0.1 g, 0.246 mM) in 20 cm^3 of toluene. The mixture was heated at reflux temperature under an inert N_2 atmosphere for 4 h. A yellow precipitate was filtered and dried overnight. It was then dissolved in CH_2Cl_2 and layered with *n*-hexane from which yellow parallelogram-shaped crystals formed.

Yield = 71%, m.p. = 301.7 – 304.6 °C. IR (ν_{max}/cm^{-1}): ν(C≡O) 2013, 1924, 1880 (vs), ν(C=O) 1636 (m), ν(C–O–C) 1620, 1609 (m), ν(C–N)$_{Heterocyclic}$ 1570 (m), ν(C–S) 760 (s); ^{1}H NMR (295 K/ppm): 9.05 (s, 1H, *H12*), 8.71 (d, 1H, *H8*), 8.51 (d, 1H, *H5*), 8.09 – 8.00 (m, 2H, *H6*, *H73*), 7.89 – 7.67 (m, 4H, *H14*, *H15*, *H16*, *H17*). UV–Vis (DMF, (λ_{max} (ε, M^{-1}cm^{-1})): 258 nm (1130); 291 nm (1030); 317 nm (766); 381 nm (sh, 362). Conductivity (DMF, 10^{-3} M): 0.596 Ohm^{-1}cm^{-2}Ml^{-1}.

2.5. *[ReO(Hns)] (2)*

The title compound was afforded from reaction of Htch (0.059 g, 0.0207 mM) with *trans*-[ReOBr$_3$(PPh$_3$)$_2$] (0.1 g, 0.0103 mM) in 20 cm^3 of refluxing MeOH for 3.5 h. The resultant reaction mixture was allowed to cool to room temperature. A maroon precipitate was filtered, dried under vacuum and then dissolved in CH_2Cl_2 and layered with *n*-hexane. From this solution reddish brown parallelogram-shaped crystals were isolated which were suitable for single crystal X-ray analysis. Yield = 52%, m.p. = >350 °C; IR (ν_{max}/cm^{-1}): ν(O–H) 3062 (w), ν(C=O) 1621, 1585, 1574 (m), ν(C=N) 1558 (m), ν(Re=O) 986 (m), ν(C–S) 749, 761 (vs); ^{1}H NMR (295K/ppm): 10.49 (br, s, 1H, O*H*), 9.28 (s, 2H, *H7*, *H8*), 7.83 – 7.71 (m, 4H, *H18*, *H19*, *H20*, *H21*), 7.51 – 7.42 (m, 2H, *H2*, *H14*), 7.32 (t, 2H, *H3*, *H4*), 7.20 (t, 2H, *H12*, *H13*), 7.10 – 7.00 (m, 2H, *H5*, *H11*). (see figure S3) UV–Vis (DMF, (λ_{max} (ε, M^{-1}cm^{-1}))): 252 nm (sh, 1320); 268 nm (sh, 1060); 281 nm (1040); 310 nm (1080); 440 nm (193). Conductivity (DMF, 10^{-3} M): 0.571 Ohm^{-1}cm^{-2}M^{-1}.

2.6. *[ReO(OCH$_3$)(PPh$_3$)(Huch)] (3)*

Equimolar ratios of H$_3$uch (0.037 g, 0.0103 mM) and *trans*-[ReOBr$_3$(PPh$_3$)$_2$] (0.1 g, 0.0103 mM) were dissolved in 20 cm^3 of MeOH and the resultant reaction mixture was refluxed for 3 h. The mother liquor was halved and both aliquots were diluted with a further 10 cm^3 of MeOH. Brown platelet crystals formed *via* slow evaporation of the mother liquor. Yield = 58%, m.p. = >350 °C. IR (ν_{max}/cm^{-1}): ν(N-H) 3039(w), ν(C=O) (sh) 1722, 1683(s), ν(C=N) 1616, 1558, 1570(s), ν(C–O–C) 1513, 1463(s), ν(O–CH$_3$) 1186(m), ν(Re=O) 1093 (m); ^{1}H NMR (295K/ppm): 9.79 (s, 1H, *H7*), 9.33 (br, s, 1H, N(1)*H*), 9.30 (s, 1H, *H9*), 8.98 (br, s, 3H, C(3)*H$_3$*), 8.51 (br, s, 3H, C(1)*H$_3$*), 8.13 (d, 1H, *H14*), 7.81 (t, 2H, *H12*, *H13*), 7.74 (d, 1H, *H11*), 7.57–7.28 (m, 15H, *PPh$_3$*), 4.17 (br, s, 3H, C(17)*H$_3$*), 1.20 (s, 3H, C(18)*H$_3$*). ^{31}P NMR (295K/ppm) 25.67. UV–Vis (DMF, (λ_{max} (ε, M^{-1}cm^{-1})): 240 nm (3590); 280 nm (2970); 344 nm (446); 401 nm (230); 473 nm (56); 766 nm (4.45). Conductivity (DMF, 10^{-3} M): 1.548 Ohm^{-1}cm^{-2}M^{-1}.

2.7. *X-ray diffraction*

X-ray data were recorded on a Bruker Apex Duo equipped with an Oxford Instruments Cryojet operating at 100(2) K and an Incoatec microsource operating at 30 W power. Crystal and structure refinement data are given in table 1. Selected bond lengths and angles are given in tables 2 and 3. The data were collected with Mo Kα (λ = 0.71073 Å) radiation at a crystal-to-detector distance of 50 mm. The following conditions were used for the data collection: omega and phi scans with exposures taken at 30 W X-ray power and 0.50° frame widths using APEX2 [23]. The data were reduced with SAINT [24] using outlier rejection,

Downloaded by [Chongqing University] at 13:34 14 February 2014

Table 1. Crystal data and structure refinement data.

	1·CH_2Cl_2	**2**	**3**
Chemical formula	$C_{20}H_{11}Cl_3NO_5ReS$	$C_{22}H_{15}O_3ReS_2$	$C_{36}H_{30}N_4O_7PReBr$
Formula weight	669.93	605.71	851.85
Temperature (K)	100(2)	100(2)	100(2)
Crystal system	Monoclinic	Monoclinic	Triclinic
Space group	$P2_1/c$	P_12_1/c_1	$P\text{-}1$
Unit cell dimensions (Å, °)	a = 10.8720(4)	a = 11.3071(5)	a = 9.7726(4)
	b = 13.9219(5)	b = 13.9167(6)	b = 12.8281(5)
	c = 14.3374(5)	c = 12.9198(5)	c = 14.3678(6)
	α = 90.00°	α = 90.00°	α = 69.801(2)°
	β = 103.687(2)°	β = 106.785(2)°	β = 86.957(2)°
	γ = 90.00°	γ = 90.00°	γ = 83.384(2)°
Crystal size (mm)	0.40 × 0.15 × 0.10	0.22 × 0.18 × 0.10	0.18 × 0.10 × 0.06
V (Å^3)	2108.47(13)	1946.41(11)	1679.00(14)
Z	4	4	2
Density (Calcd) (Mg/m^3)	2.11	2.07	1.68
Absorption coefficient (mm^{-1})	6.277	6.486	3.723
F (000)	1279.7	1167.7	839.8
θ Range for data collection (°)	1.9; 26.4	3.6; 28.3	5; 27.0
Index ranges	$-13 \le h \le 13$	$-13 \le h \le 15$	$-7 \le h \le 11$
	$-14 \le k < 17$	$-15 \le k < 18$	$-14 \le k < 16$
	$-17 \le l \le 17$	$-17 \le l \le 13$	$-18 \le l \le 17$
Reflections measured	17401	13794	16569
Observed reflections [I>2σ(I)]	3965	4452	6143
Independent reflections	4237	4798	6620
Data/restraints/parameters	4237/0/275	4798/0/278	6620/0/445
Goodness of fit on F^2	1.077	1.261	1.142
Observed R, wR^2	0.017; 0.039	0.015; 0.045	0.101; 0.095
R_{int}	0.015	0.019	0.015

Table 2. Selected bond lengths [Å] and angles [°] for **1**.

	Experimental	Optimized
Re–C1	1.923(3)	1.916
Re–C2	1.900(3)	1.905
Re–C3	1.922(3)	1.922
Re–N	2.210(2)	2.266
Re–O4	2.147(2)	2.211
Re–Cl1	2.4605(7)	2.510
C10–N	1.314(4)	1.312
C10–S	1.738(3)	1.762
C9–S	1.730(3)	1.743
C4–N	1.399(4)	1.400
C10–C11	1.469(4)	1.466
C11–C12	1.362(4)	1.362
C19–O4	1.256(3)	1.242
C16–C17	1.377(4)	1.382
C1–Re–Cl1	176.68(8)	175.95
C2–Re–O4	175.0(1)	173.95
C3–Re–N	173.0(1)	172.03
O4–Re–N	82.24(8)	81.03
C10–N–C4	111.5(2)	111.90
N–C4–C5	127.0(3)	126.81

Downloaded by [Chongqing University] at 13:34 14 February 2014

Table 3. Selected bond lengths [Å] and angles [°] for **2** and **3**.

2			**3**		
	Experimental	Optimized		Experimental	Optimized
Re–O1	1.684(2)	1.686	Re–O1	1.697(4)	1.703
Re–N1	2.080(2)	2.104	Re–O2	1.918(4)	1.941
Re–N2	2.083(2)	2.098	Re–O3	2.109(4)	2.165
Re–S1	2.2848(7)	2.314	Re–N1	2.000(5)	2.013
Re–S2	2.2892(6)	2.318	Re–N4	2.087(5)	2.080
C7–N1	1.335(3)	1.329	Re–P	2.457(2)	2.553
C9–N2	1.331(3)	1.333	N4–C7	1.305(9)	1.320
C7–C8	1.399(3)	1.396	C8–C9	1.51(1)	1.507
C8–C9	1.402(3)	1.401	C8–C16	1.394(8)	1.403
C16–O2	1.238(4)	1.240	C15–C16	1.472(9)	1.473
C22–O3	1.358(4)	1.338	C16–O3	1.300(8)	1.288
O1–Re–N1	108.65(8)	106.88	C9–O5	1.403(8)	1.402
O1–Re–S1	108.07(7)	109.72	C17–O5	1.43(1)	1.425
O1–Re–N2	105.29(8)	108.45	O1–Re–O2	168.3(2)	166.83
O1–Re–S2	108.99(7)	108.97	O3–Re–N1	168.3(2)	168.40
N1–Re–N2	87.10(8)	83.31	N4–Re–P	170.1(1)	171.68
N1–Re–S1	82.31(6)	81.96	N1–Re–N4	79.3(2)	79.37
N2–Re–S2	82.48(6)	82.00	N4–Re–O3	91.9(2)	90.73
C7–C8–C9	124.1(2)	124.19	C5–N4–C7	124.4(5)	123.54
N1–Re–S2	142.35(6)	144.15	C18–O2–Re	140.0(4)	146.43
N2–Re–S1	146.64(6)	141.84	C17–O5–C9	114.5(6)	114.41
Re–N1–C7	121.0(2)	121.27	–	–	–
Re–N2–C9	120.0(2)	119.92	–	–	–

Downloaded by [Chongqing University] at 13:34 14 February 2014

scan speed scaling, as well as standard Lorentz and polarization correction factors. A SADABS semi-empirical multi-scan absorption correction [25] was applied to the data. Direct methods, SHELXS-97 [26] and WinGX [27] were used to solve all three structures. All non-hydrogen atoms were located in the difference density map and refined anisotropically with SHELXL-97 [26]. All hydrogens were included as idealized contributors in the least squares process. Their positions were calculated using a standard riding model with C–$H_{aromatic}$ distances of 0.93 Å and U_{iso} = 1.2 Ueq. The CH_2Cl_2 solvate C–H bonds of **1**, the phenolic O–H bonds of **2** and amido N–H bond of **3** were located in the difference density map and refined isotropically.

2.8. *Computational details*

Computational calculations were conducted with Gaussian 09W [28]. Geometry optimizations of the rhenium complexes were achieved through DFT calculations using the B3LYP functional, with an accompanying hybrid basis set *viz.* the 6-311G^{++} (*d, p*) basis set was applied to all the C, H, N, O, and S (for **1** and **2**)/P (for **3**) atoms and the LANL2DZ basis set applied to the metal centre [11, 29]. The crystal structures were used as starting structures but the CH_2Cl_2 solvent (for **1**) of recrystallization was removed prior to any calculations. Good agreement was found between the optimized and geometrical parameters (refer tables 2 and 3) with the minor deviations due to the fact that gas phase optimized structures do not account for hydrogen bonding interactions or any short distance contacts. Using the optimized structures of the metal complexes, frequency calculations confirmed that the respective structures are at global minima on the potential energy surfaces and from these, reliable vibrational energies were attained [30].

Downloaded by [Chongqing University] at 13:34 14 February 2014

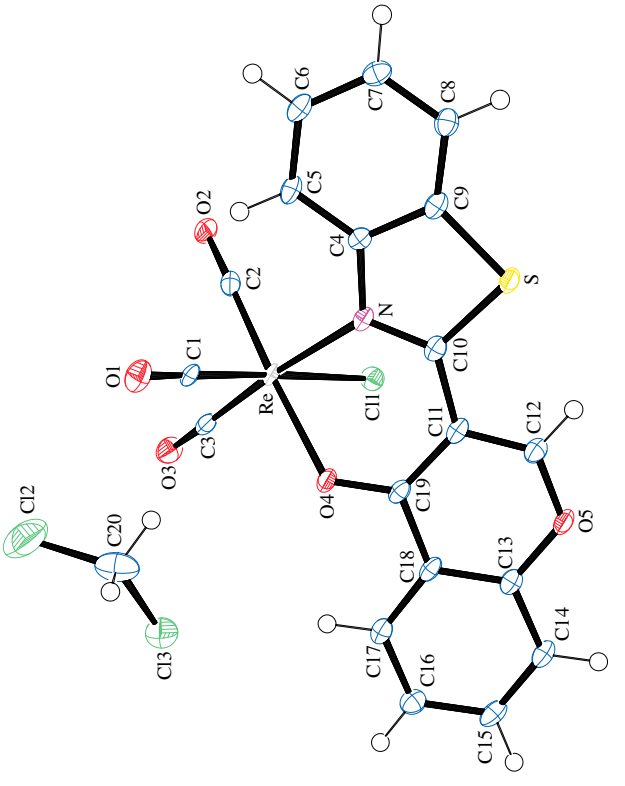

Figure 1. An ORTEP view of **1**·CH_2Cl_2 showing 50% probability displacement ellipsoids and the atom labelling.

3. Results and discussion

3.1. *Synthesis, spectral characterization and DFT studies of the rhenium complexes*

In the formation of *fac*-[$Re^{I}(CO)_3$(bsch)Cl] (**1**) (figure 1), the Schiff base Htch underwent cyclization between the thiol sulfur and the imino carbon (C10) to afford the neutral bidentate chelator, bsch. In a previous study, we observed a similar phenomenon whereby the Schiff base ligand, 2-(2-aminophenyliminomethyl)-4*H*-chromen-4-one (H_2pch) cyclized in a similar manner upon coordination to the *fac*-[$Re(CO)_3Cl$] moiety, to afford the heterocyclic, 2-benzimidazole-4*H*-chromen-4-one (bzch) chelator [31]. However, the Schiff base Htch transformed upon reacting with the more acidic rhenium(V) precursor, *trans*-[$Re^{V}OBr_3(PPh_3)_2$], which led to formation of the square pyramidal oxorhenium(V) complex, [ReO(Hns)] (**2**) (figure 2).

Upon reacting H_3uch with *trans*-[$Re^{V}OBr_3(PPh_3)_2$], [$Re^{V}O(OCH_3)(PPh_3)$(Huch)] (**3**) (figure 3) was isolated, where Huch acted as a dianionic tridentate chelator through the anionic enol oxygen O3, neutral imino nitrogen N4, and singly deprotonated amido N1 nitrogen. It was no surprise that a methoxy group covalently linked to the 2-position (i.e. C9) of the chromone moiety. A mechanism has previously been proposed for the nucleophilic addition of an ethoxy group to the same carbon position of 3-formylchromone [17, 18].

Downloaded by [Chongqing University] at 13:34 14 February 2014

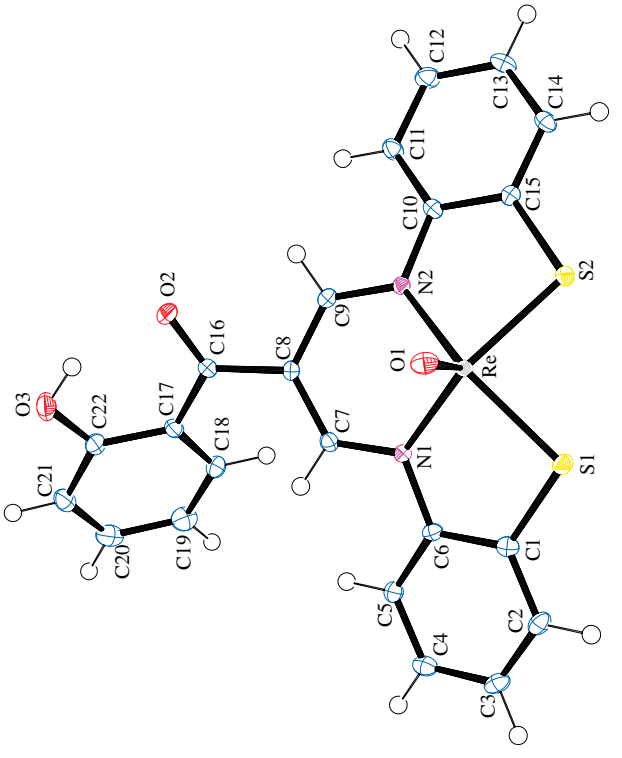

Figure 2. An ORTEP view of **2** showing 50% probability displacement ellipsoids and the atom labelling.

All the compounds exhibit good solubility in most polar solvents but moderate to non-solubility in non-polar solvents. These rhenium compounds have significantly low molar conductivity values due to their charge neutrality. The ^{1}H NMR spectra show well-resolved peaks due to the diamagnetic nature for the d^2 (for **2** and **3**) systems. Despite increasing the number of scans and using deuterated chloroform or dimethylsulfoxide, no informative ^{1}H NMR spectrum could be attained for the diamagnetic, d^6 system (complex **1**). Nevertheless, an interpretable ^{1}H NMR spectrum of **1** could be attained in deuterated dichloromethane. In comparison to the spectrum of the free ligand (i.e. Htch), the spectrum of **1** indicates there are no signals found for the protons associated with the mercapto and Schiff base imino groups. Also, selected aromatic peaks of the bsch chelator coalesce into two multiplets which integrates to two (between 8.09 – 8.00 ppm) and four (between 7.89 – 7.67 ppm) protons, respectively. The remaining signals of **1** appear downfield as two doublets, which are assigned to the aromatic protons on the benzothiazole moiety, and a sharp singlet, due to the proton (H12) of the chromone moiety. For **2**, the hydrogens of the bridging phenyl ring occur as a four proton multiplet and the proton of the phenolic oxygen appears as a broad singlet (at 10.49 ppm). The remaining proton signals emphasize symmetry within the molecule, e.g. only one sharp signal appears for the Schiff base hydrogens which integrates for two (see figure S3). A distinctive feature of the ^{1}H NMR spectrum of **3** is the sharp singlet at 4.17 ppm which is assigned to the three protons of the methoxy group covalently bonded to the chromone moiety. The methine proton was found as a singlet at 9.79 ppm

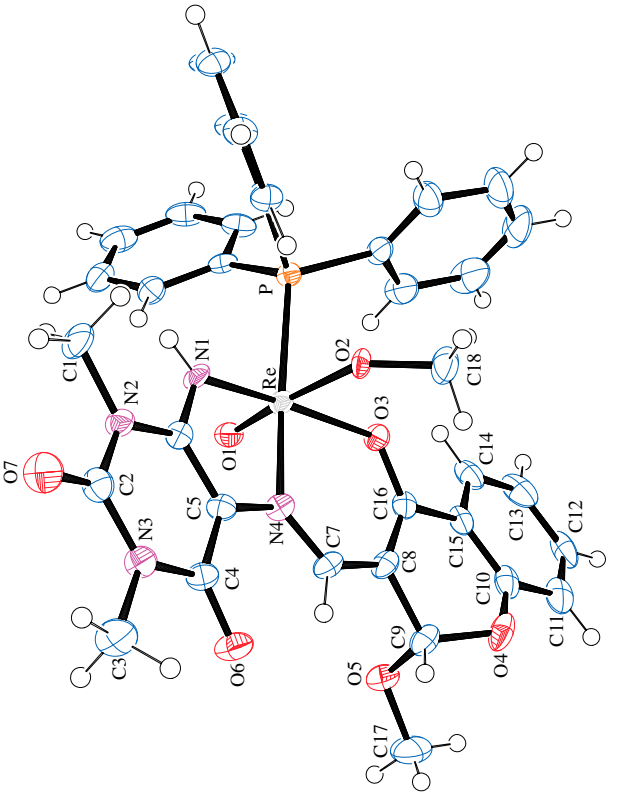

Figure 3. An ORTEP view of **3** showing 50% probability displacement ellipsoids and the atom labelling.

and is found at a similar position relative to the imine proton of the free ligand H_3uch (at 9.78 ppm). Furthermore, the proton of the singly deprotonated amino group is found at 9.33 ppm and this signal integrates to one proton. This signal is a clear indication that coordination has occurred since in the free-ligand's ^{1}H NMR spectrum the signal of the amino proton's signal appears as a broad singlet at 7.41 ppm (figure S2). This was also accompanied by the disappearance of the hydroxyl proton of the chromone group.

The IR spectrum of **1** is dominated by the intense bands of the tricarbonyl co-ligands (2013, 1924 and 1880 cm^{-1}), while a strong vibrational band is found at 760 cm^{-1} due to *ν*(C–S). All other bands associated with the chromone and heterocyclic moieties are found as medium intensity bands between 1636 and 1570 cm^{-1} (figure S4). In the IR spectrum of **2**, the hydroxyl vibration appears as a weak intensity band at 3062 cm^{-1}. No ether vibrational bands were found for **2** (compared to the *ν*(C–O–C) bands at 1620 and 1609 cm^{-1} for **1**) due to transformation of the chromone. The three medium intensity ketonic vibrational bands at 1621, 1585 and 1574 cm^{-1} are further evidence that the ligand has transformed. The two bands due to *ν*(C=N) overlap and appear as a broad vibrational band (1558 cm^{-1}), while the two C–S vibrations appear individually as sharp and strong bands at 749 and 761 cm^{-1}. The vibrational peaks at 986 (for **2**) and 917 (for **3**) cm^{-1} are found in the 890 – 1020 cm^{-1} range [32] and are ascribed to rhenium(V)-oxo stretching vibrations. The optimized and experimental (see figures S4 and S5) IR spectra of **1** showed distinctive

Downloaded by [Chongqing University] at 13:34 14 February 2014

similarities. For example in **1**, intense vibrations associated with the *fac*-$[Re(CO)_3]^+$ core are computed at 2101, 2020 and 1995 cm^{-1} (figure S5), while a medium intensity band is computed at 1659 cm^{-1} which constitute the main vibrations as induced by the heterocyclic and chromone moieties. However, for **2** the calculated $[Re^{V}O]^{3+}$ core vibrates at a much higher frequency (observed at 1021 cm^{-1}) than what was experimentally (at 986 cm^{-1}) observed (figure S6). This is largely ascribed to the fact that the gas phase frequency calculation of **2** does not account for weak inter- and intramolecular interactions as observed within the crystal structure. This was also observed in the deviation of the calculated (observed at 3411 cm^{-1}) and experimental hydroxyl group vibrational bands (observed at 3062 cm^{-1}), where the aforementioned is also influenced by the classical hydrogen-bonding between the ketonic oxygen and the hydroxyl group.

Multiple vibrations were found in the IR spectrum of **3**, resulting in considerable overlapping of the vibrational bands, whereby many bands coalesced into broad bands or into bands with poor resolution. However, a weak intensity band at 3039 cm^{-1} was clearly observed and is assigned to ν(N–H). A frequency calculation of the optimized structure provided insight into the interpretation of the experimental IR spectrum of **3** (figure 4). Similar ketonic vibrational frequencies of the uracil moiety were found between the experimental (a shoulder at 1772 cm^{-1} and a strong vibration at 1683 cm^{-1}) and optimized molecules (1741 and 1696 cm^{-1}). Similarly, the ν(C=N) vibrational bands appear as three peaks in both the calculated (1588, 1633 and 1642 cm^{-1}) and experimental (1570, 1588 and 1616 cm^{-1}) spectra. The peaks between 1450 and 1550 cm^{-1} in the calculated spectrum are largely due to the vibrations associated with the chromone moiety [i.e. ν(C–O–C)], and similarly in the corresponding region of the experimental spectrum, two bands (1463 and 1513 cm^{-1}) were found. Medium intensity bands were experimentally observed for the

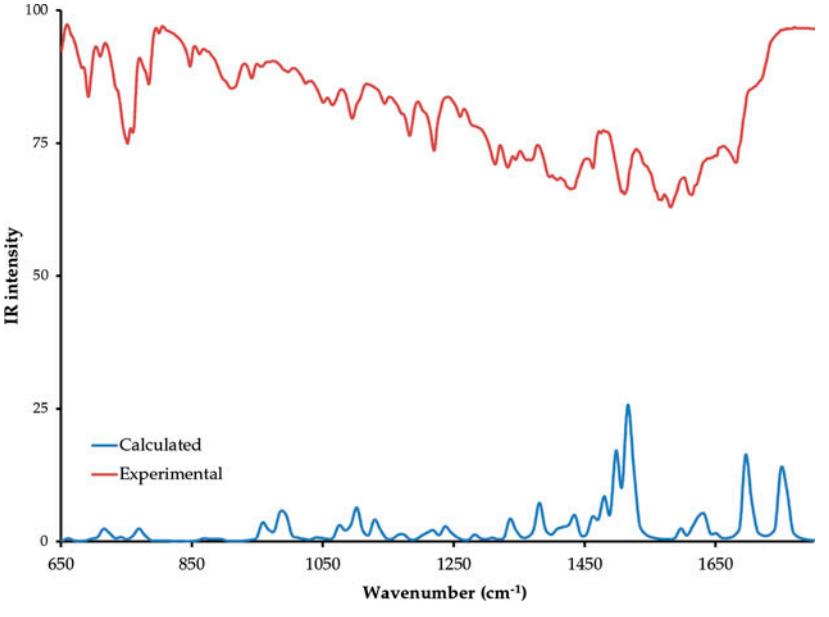

Figure 4. Experimental (red) and calculated (blue) IR spectra of **3**. Note that the calculated spectrum is not plotted to scale (see http://dx.doi.org/10.1080/00958972.2013.867028 for color version).

Downloaded by [Chongqing University] at 13:34 14 February 2014

Downloaded by [Chongqing University] at 13:34 14 February 2014

metal to oxo (1093 cm^{-1}) and metal to methoxy (1186 cm^{-1}) bonds which were assigned based on the calculated vibrations at 1137 [Re(V)=O] and 1176 cm^{-1} [Re(V)–OCH_3]. These rhenium to oxygen vibrational bands were similar to other compounds with Re(V)=O and Re(V)-OCH_3 bonds [33]. The close correlation between the optimized and geometrical parameters of the respective complexes is further emphasized by the low calculated RMSD values (figure 5). The larger RMSD value of **3** is mainly attributed to the flexible degree of rotation of the P-C single bonds within the PPh_3 co-ligands.

The electronic spectra of **1** and **2** exhibit similar electron transitions in comparison to the electronic spectrum of the free ligand (Htch) (see figure S7). Therefore, the electronic transitions within the UV region (but below 375 nm) were assigned to π–π* transitions (258, 291, 317 nm for **1** and 252, 268, 281, 310 nm for **2**). The similarities are due to the highly delocalized nature of the free ligand, Htch, and chelators, bsch (for **1**) and Hns (for **2**). A ligand-to-metal charge transfer band (LMCT) is observed at 381 nm for **1** while for **2**, a metal-to-ligand charge transfer (MLCT) band at 440 nm is observed. Indicative to **1** and **2**, **3** showed an array of π-π* transitions (240, 280 and 344 nm) in addition to two MLCT bands at 401 and 473 nm. No d-d transition was observed for **1** due to its low-spin d^6 electron configuration whereas the oxorhenium(V) complex **3** had a distinctive d-d transition (but with a low extinction coefficient) due to its d^2 configuration. No metal-based electronic transition could be observed for the other oxorhenium(V) compound **2**.

3.2. *Crystal structure of 1·CH_2Cl_2*

Compound **1** exhibits a distorted octahedral geometry which is largely due to the six-membered chelate [Re, O4, C19, C11, C10, N] ring which affords a constrained bite angle of 82.24(8)° [O4–Re–N] (figure 1). This phenomenon induces larger deviations from linearity within the equatorial angles (N–Re–C3 = 173.0(1)° and O4–Re–C2 = 175.0(1)°) compared to the axial angle [C1–Re–Cl1] of 176.68(8)°.

Evaluating the bonds within the coordination sphere, the Re–C2 bond (1.900(3) Å) has a significantly shorter bond distance than the other metal carbon bonds (Re–C1 = 1.923(3) Å and Re–C3 = 1.922(3) Å). This is accounted to the weaker *trans*-influence of the ketonic oxygen O4 compared to the N donor atom and Cl1 co-ligand. All the other coordination

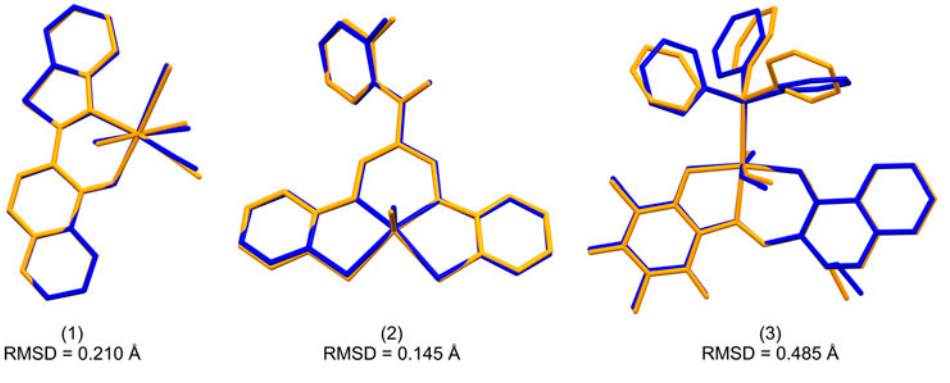

Figure 5. Overlay structures of the optimized and crystal structures for the respective complexes with their corresponding RMSD values. The crystal structures are shown in blue while the optimized structures are given in yellow (see http://dx.doi.org/10.1080/00958972.2013.867028 for color version).

sphere bonds within **1** were comparable with similar rhenium(I) compounds as found in the literature. For example, the metal-ketonic oxygen (Re–O4 = 2.147(2) Å) and chloride (Re–Cl1 = 2.4605(7) Å) bond lengths were similar to the bonds of the benzimidazole analogue, *fac*-[Re^{I}(CO)$_3$Cl(bzch)] {Re-O$_{ketonic}$ = 2.137(2) Å and Re–Cl1 = 2.492(6) Å} [31]. The Re-N distance of 2.210(2) Å was in the range of rhenium(I) compounds with coordinating benzothiazole moieties [34, 35]. For example, in *fac*-[Re^{I}(Habt)(CO)$_3$Br], where the 2-aminophenyl-1*H*-benzothiazole (Habt) coordinated in an analogues manner (i.e. as a neutral bidentate chelator within the equatorial plane), a rhenium imidazolium bond distance of 2.227(2) Å was observed [36].

Within the benzothiazole moiety, the bond orders of the C–N bonds are readily distinguishable based on their distances (C10–N = 1.314(4) Å and C4–N = 1.399(4) Å). In contrast to the C–N bond distance, the C–S single bonds (C9–S = 1.730(3) Å and C10–S = 1.738(3) Å) are nearly equidistant. It was found that the C11-C12 (1.362(4) Å) double bond has a similar bond length as the delocalized C–C double bonds (e.g. C16–C17 = 1.377(4) Å) within the phenyl ring, showing unequivocally that it is a localized double bond.

The chromone and benzothiazole moieties are bridged by a carbon-carbon (C10-C11 = 1.469(4) Å) single bond which allows the moieties to form a dihedral angle of 7.95°. In turn, these moieties are found considerably out of the mean equatorial plane by 34.72° (for benzothiazole) and 36.84° (for chromone). The crystal lattice is stabilized by a dichloromethane (CH_2Cl_2) solvent molecule which interacts *via* non-classical hydrogen-bonds with a molecule of **1**. Further stabilization is afforded through intermolecular π-π* bonding between the bsch chelators of adjacent molecules with a distance of 3.729 Å between two opposing conjugated phenyl rings. Each unit cell consists of four molecules of **1** with their corresponding dichloromethane solvent molecule of recrystallization. Furthermore, the bsch chelator of each molecule aligns with the [*b*]-axis (see figure S8).

Facial tricarbonyl rhenium(I) complexes with benzothiazole-based chelators are well documented [34–38]. A typical example is *fac*-[Re(CO)$_3$(bt)$_2$Cl], which was isolated from the 2 : 1 molar ratio reaction of benzothiazole (bt) with [Re(CO)$_5$Cl] in anhydrous methanol. The two bt chelators coordinated as two neutral monodentate chelators [37]. Recently, the isolation of a unique dinuclear rhenium(I) compound, (μ-dbt)$_2$[Re(CO)$_3$]$_2$, [Hdbt = *bis*-{1,2-(benzothiazol-2-ylidene)}thiourea] was reported. The complex contains two *fac*-[Re(CO)$_3$]$^+$ moieties and two bridging anionic tridentate chelators dbt which coordinates individually in a bidentate manner to one metal center but also monodentate to the other metal center [38].

3.3. *Crystal structure of 2*

Compound **2** exhibits a square-pyramidal geometry with the rhenium-oxo core occupying the apical position relative to the tetradentate N_2S_2 chelator (Hns) in the equatorial plane (figure 2). However, the structure is highly distorted as the Re atom lies 0.664 Å out of the mean equatorial plane [N1, N2, S1, S2], which affords large deviations from the idealized 90° for the angles: O1–Re–N1 = 108.65(8)°, O1–Re–N2 = 105.29(8)°, O1–Re–S1 = 108.07(7)° and O1–Re–S2 = 108.99(7)°. Another contributive factor to the distortion is the influence of the five- and six-membered chelate rings which affords constrained bite angles (N1–Re–S1 = 82.31(6)°, N1–Re–N2 = 87.10(8)° and N2–Re–S2 = 82.48(6)°) which are smaller than the idealized angle (90°).

Downloaded by [Chongqing University] at 13:34 14 February 2014

Downloaded by [Chongqing University] at 13:34 14 February 2014

The Re–N1–C7 (121.0(2)°) and Re–N2–C9 (120.0(2)°) angles emphasize the sp^2-hybridization of the N1 and N2 atoms. The hybridization of the nitrogens is further supported by the Schiff base bond distances (C7–N1 = 1.335(3) Å and C9–N2 = 1.331(3) Å), which were comparable to other chelating Schiff base moieties coordinated to the oxorhenium(V) core [39]. Interestingly, the bridging carbon to carbon bond distances (C7–C8 = 1.399(3) Å and C8–C9 = 1.402(3) Å) have similar bond distances compared to those found within the phenyl rings (e.g. C5–C6 = 1.401(3) Å). Of further interest is that these bridging carbons afford a bond angle of C7–C8–C9 = 124.1(2)°, which is close to the bond distances and angles found in the para-diazabenzenesulfonic complexes, [M(oyl)-N=N-$C_6H_4SO_3H$] {M = Ni or CuH, oyl = 1,1,2,8,9,9-hexamethyl-4,6-dioxa-5-hydro-3,7,10,14-tetraazacyclotetradecane-2,7,10,12-tetraene}, containing an analogous aliphatic sp^2 NCCCN bridged moiety [40]. This implies that the bridging carbon to carbon bonds are delocalized double bonds and that the C7–C8–C9 bridge acts as a delocalized anionic moiety. This affirms that the Hns chelator acts as a tri-anionic tetradentate chelator.

The phenolic bond distance (C22–O3 = 1.358(4) Å) is much longer than the ketonic bond distance (C16–O2 = 1.238(4) Å), which indicates that the latter is a double bond. In addition, one intramolecular classical hydrogen-bond is observed between the above-mentioned moieties (O3–H11···O2 = 1.87(4) Å). Despite the highly delocalized nature of the Hns chelator, no intermolecular π–π stacking was observed.

Although oxorhenium(V) complexes adopting square pyramidal geometries are common in literature [41–43], rhenium complexes with a delocalized monoanionic carbon bridged system could not be found. A neutral square pyramidal complex [ReO(dne)], H_3dne = *N′*-(2-aminobenzyl)-*N*-[(2-aminophenyl)methylidene]ethane-1,2-diamine and its complex salt derivative, [ReO(ane)]PF_6 were formed from the reactions of the symmetrical diimine ligand *N,N′-bis*-(2-aminophenyl)methylidene]ethane-1,2-diamine (H_2ane) with *trans*-[$Re^{V}O_2(py)_4$]Cl and *cis*-[$ReO_2I(PPh_3)_2$], respectively. The chelator dne {in [ReO(dne)]} acts as a triamido imine in which one imine group is reduced upon coordination whereas for [ReO(ane)]PF_6 the ane chelator acts as a dimino diamido moiety [44]. Furthermore, several square pyramidal oxorhenium(V) complexes with a '3+1' mixed-ligand coordination behavior have been reported. The motivation behind this design is that it limits the formation of multiple isomers with different biological activity, which is commonly found for the tetradentate chelated oxorhenium(V) complexes. An additional advantage is that a biologically active molecule can be covalently conjugated to either the tri- or mono-organic ligands within the coordination sphere or directly coordinated to the metal center [45–47].

3.4. *Crystal structure of 3*

The six-coordinate complex, [ReO(OCH_3)(PPh_3)(Huch)], was isolated as XRD quality brown plates, grown from slow evaporation of the mother liquor**.** Two crystallographically dependent molecules of **3** occupy the asymmetric unit cell in the space group P-1, i.e. Z = 2 (see figure S9). The rhenium metal atom is in the center of a distorted octahedron with the dianionic tridentate chelator, Huch, and the PPh_3 co-ligand occupying the equatorial plane, while the axial is formed by the metal oxo (Re=O) moiety and the methoxy [O2–C18H_3] co-ligand (figure 3). The octahedral distortion is brought about by five- and six-membered chelate rings with bite angles of 79.3(2)° [N1–Re–N4] and 91.9(2)° [O3–Re–N4], which induce deviations from linearity for the angles: O1–Re–O2 = 168.3 (2)°, N4–Re–P = 170.1(1)° and O3–Re–N1 =168.3(2)°.

The enol form of the ligand in **3** is confirmed from the longer C–O distance (C16–O3 = 1.300(8) Å) compared to the ketone bond distances in **1** (C19–O4 = 1.256(3) Å) and **2** (C16–O2 = 1.238(4) Å). The presence of the enol tautomer is further supported by the significantly different C–C (C8–C16 = 1.394(8) Å and C15–C16 = 1.472(9) Å) bonds within the chromone moiety, which is indicative of variable bond orders. Similar rhenium(V)-oxo bond lengths were found for **2** (Re–O = 1.684(2) Å) and **3** (Re–O1 = 1.697(4) Å). The C7–N4–C5 bond angle of 124.4(5)° deviates from the ideal 120° expected for a bond angle containing a bridging sp^2-hybridized nitrogen, which is largely ascribed to the influence of the five-membered chelate ring. However, the Re–N4 bond distance of 2.087(5) Å is well within the expected range (2.03(1) – 2.15(1) Å) for rhenium(V) compounds containing Schiff base chelates [48–50]. The other rhenium to nitrogen coordination bond, Re–N1 (2.000(5) Å), is close to the lower end of the literature range (1.91(1) – 2.01(1) Å) found for rhenium(V)-amido bonds [51–55]. As expected, the rhenium methoxy (Re–O2 = 1.918(4) Å) bond length in **3** is much longer than the rhenium oxo bonds (for **2** and **3**) but similar to other Re(V)–O–CH_3 bond distances typically observed for oxorhenium(V) compounds [56, 57]. In addition, the Re-P bond distance of 2.457(2) Å is almost identical to that found in the *p*-tolylimido (*p*-$NC_6H_4CH_3$) rhenium(V) complex salt, [Re(*p*-$NC_6H_4CH_3$)(hpb)$_2$(PPh_3)]Cl, Hhpb = 2-(2-hydroxyphenyl)-1*H*-benzimidazole {Re–P = 2.460(2) Å} [58].

4. Conclusion

The coordination behavior of the chromone derived Schiff bases towards the *fac*-$[Re^{I}(CO)_3]^+$ and $[Re^{V}O]^{3+}$ cores resulted in formation of metal complexes with unique structural features. For **1**, *fac*-[$Re^{I}(CO)_3$(bsch)Cl], the bsch chelator, shared the same proposed pathway of formation and coordination mode as the analogous heterocyclic, 2-benzimidazole-4*H*-chromen-4-one (bzch) chelator found in a previously isolated rhenium(I) compound, *fac*-[Re$(CO)_3$(bzch)Cl]. Similarly, in **3**, [ReO(OCH_3)(PPh_3)(Huch)], the Huch chelator, coordinated as a dianionic tridentate moiety through the singly deprotonated uracil amido nitrogen and the classical chromone Schiff base $N_{imino}O_{enol}$ donor set which is common to other tridentate chromone Schiff bases coordinated to transition metal complexes. For **2**, the manner in which Htch transformed was not previously observed for this class of ligands. The resultant complexes were spectroscopically characterized and their structures confirmed by single crystal X-ray diffraction. Optimized and experimental geometrical parameters of the complexes are in reasonable agreement. Furthermore, the computed vibrational properties of the complexes have similarities to that of the respective experimental IR spectra. Future prospects entail anticancer-activity testing against various cell-lines and the compounds that exhibit optimal cytotoxicity may proceed to radiopharmaceutical studies.

Supplementary material

CCDC 940580, 940578 and 940578 contains the supplementary crystallographic data for **1**·CH_2Cl_2, **2** and **3**. These data can be obtained free of charge at www.ccdc.cam.ac.uk/conts/retrieving.html [or from the Cambridge Crystallographic Data Centre (CCDC), 12 Union Road, Cambridge CB2 1EZ, UK; Fax: +44(0)1223-336033; or E-mail: deposit@ccdc.cam.ac.uk].

Downloaded by [Chongqing University] at 13:34 14 February 2014

Acknowledgements

We are grateful to the University of KwaZulu-Natal and the National Research Foundation of South Africa for financial support.

References

[1] J.R. Dilworth, S.J. Parrott. *Chem. Soc. Rev.*, **27**, 43 (1998).
[2] U. Abram, R. Alberto. *J. Braz. Chem. Soc.*, **17**, 1486 (2006).
[3] W. Wang, B. Spingler, R. Alberto. *Inorg. Chim. Acta*, **355**, 386 (2003).
[4] K. Potgieter, P. Mayer, T. Gerber, N. Yumata, E. Hosten, I. Booysen, R. Betz, M. Ismail, B. van Brecht. *Polyhedron*, **49**, 67 (2013).
[5] I. Booysen, T.I.A. Gerber, E. Hosten, P. Mayer. *Inorg. Chem. Commun.*, **11**, 33 (2008).
[6] X. Chen, F.J. Femia, J.W. Babich, J. Zubieta. *Inorg. Chim. Acta*, **33**, 316 (2001).
[7] T.I.A. Gerber, N.C. Yumata, R. Betz. *Inorg. Chem. Commun.*, **15**, 69 (2012).
[8] C. Lin, H. Pan, V.N. Nesterov, M.G. Richmond. *J. Organomet. Chem.*, doi.org/10.1016/j.jorganchem.2013.03.049 (2013).
[9] M.M. Mashaly. *J. Coord. Chem.*, **48**, 165 (1999).
[10] D.A. Rotsch, K.M. Reinig, E.M. Weis, A.B. Taylor, C.L. Barnes, S.S. Jurisson. *Dalton Trans.*, (2013). doi:10.1039/C3DT51198G.
[11] A. Brink, H. Visser, A. Roodt. *Polyhedron*, **52**, 416 (2013).
[12] C.M. da Silva, D.L. da Silva, L.V. Modolo, R.B. Alves, M.A. de Resende, C.V.B. Martins, Â. de Fátima. *J. Adv. Res.*, **2**, 1 (2011).
[13] K. Sztanke, A. Maziarka, A. Osinka, M. Sztanke. *Bioorg. Med. Chem.*, **21**, 3648 (2013).
[14] M.L. Ferreira, T.R.A. Vasconcelos, E.M. de Carvalho, M.C.S. Lourenço, S.M. Wardell, J.L. Wardell, V.F. Ferreira, M.V.N. de Souza. *Carbohydr. Res.*, **344**, 2042 (2009).
[15] C. Liu, Z. Yang, M. Yan. *J. Coord. Chem.*, **65**, 3845 (2012).
[16] K.M. Khan, N. Ambreen, S. Hussain, S. Perveen, M.I. Choudhary. *Bioorg. Med. Chem.*, **17**, 2983 (2009).
[17] M. Kalanithi, D. Kodimunthiri, M. Rajarajan, P. Tharmaraj. *Spectrochim, Acta, Part A*, **52**, 290 (2011).
[18] T. Ruso, E. Pahunto, C. Maxim, R. Georgescu, N. Stanica, G.L. Almajan, A. Gulea. *Polyhedron*, **29**, 757 (2010).
[19] Y. Li, Z. Yang, Z. Liao, Z. Han, Z. Liu. *Inorg. Chem. Commun.*, **13**, 1213 (2010).
[20] Y. Li, Z. Yang, JWu Eur. *J. Med. Chem.*, **45**, 5692 (2010).
[21] Q. Wang, Z. Yang, G. Qi, D.D. Qin. *Eur. J. Med. Chem.*, **44**, 2425 (2009).
[22] B. Wang, Z. Yang, M. Lü, J. Hai, Q. Wang, Z. Chen. *J. Organomet. Chem.*, **694**, 4069 (2009).
[23] N.P. Johnson, C.J.L. Lock, G. Wilkinson. *Inorg. Synth.*, **145**, 9 (1967).
[24] Bruker APEX2, SAINT and SADABS. Bruker AXS Inc. *Madison*., Wisconsin, USA (2010).
[25] R.H. Blessing. *Acta Cryst.*, **A51**, 33 (1995).
[26] G.M. Sheldrick. *Acta Cryst.*, **A64**, 112 (2008).
[27] L.J. Farrugia. *J. Appl. Cryst.*, **45**, 849 (2012).
[28] M.J. Frisch, G.W. Trucks, H.B. Schlegel, G.E. Scuseria, M.A. Robb, J.R. Cheeseman, G. Scalmani, V. Barone, B. Mennucci, G.A. Petersson, H. Nakatsuji, M. Caricato, X. Li, H.P. Hratchian, A.F. Izmaylov, J. Bloino, G. Zheng, J.L. Sonnenberg, M. Hada, M. Ehara, K. Toyota, R. Fukuda, J. Hasegawa, M. Ishida, T. Nakajima, Y. Honda, O. Kitao, H. Nakai, T. Vreven, J.A. Montgomery Jr, J.E. Peralta, F. Ogliaro, M. Bearpark, J.J. Heyd, E. Brothers, K.N. Kudin, V.N. Staroverov, R. Kobayashi, J. Normand, K. Raghavachari, A. Rendell, J.C. Burant, S.S. Iyengar, J. Tomasi, M. Cossi, N. Rega, J.M. Millam, M. Klene, J.E. Knox, J.B. Cross, V. Bakken, C. Adamo, J. Jaramillo, R. Gomperts, R.E. Stratmann, O. Yazyev, A.J. Austin, R. Cammi, C. Pomelli, J.W. Ochterski, R.L. Martin, K. Morokuma, V.G. Zakrzewski, G.A. Voth, P. Salvador, J.J. Dannenberg, S. Dapprich, A.D. Daniels, Ö. Farkas, J.B. Foresman, J.V. Ortiz, J. Cioslowski, D.J. Fox. Gaussian 09 (Revision A.01), Gaussian Inc., Wallingford, CT (2009).
[29] B. Machura, R. Kruszynski. *Polyhedron*, **26**, 3686 (2007).
[30] K.C. Potgieter, T.I.A. Gerber, R. Betz, L. Rhyman, P. Ramasami. *Polyhedron*, **59**, 91 (2013).
[31] I.N. Booysen, M.B. Ismail, Q.O. Munro. *Inorg. Chem. Commun.*, **30**, 168 (2013).
[32] B. Terfassa, P. Traar, M. Volpe, N.C. Mösch-Zanetti, V.J.T. Raju. Negussie Megersa, *N. Retta. Eur. J. Inorg. Chem.*, 4434 (2011).
[33] S.R. Chiozzone, R. Gonzalez, C. Kremer, G. De Munno, J. Faus. *Inorg. Chim. Acta*, **325**, 203 (2001).
[34] R. Czerwieniec, A. Kapturkiewicz, J. Nowacki. *Inorg. Chem. Commun.*, **8**, 1101 (2005).
[35] B. Machura, M. Wolff, I. Gryca, R. Kruszynski. *Polyhedron*, **40**, 93 (2012).
[36] I.N. Booysen, T.I.A. Gerber, P. Mayer. *Inorg. Chim. Acta*, **363**, 1292 (2010).
[37] B. Machura, M. Wolff, E. Benoist, Y. Coulais. *J. Organomet. Chem.*, **724**, 82 (2013).
[38] K.C. Potgieter, T.I.A. Gerber, E. Hosten. *Inorg. Chem. Commun.*, **24**, 231 (2012).
[39] I.N. Booysen, M. Ismail, T.I.A. Gerber, M. Akerman, B. Van Brecht. *S. Afr. J. Chem.*, **65**, 174 (2012).

Downloaded by [Chongqing University] at 13:34 14 February 2014

[40] R.K. Murmann, J. Chipley, P. Droege. *J. Chem. Cryst.*, **28**, 465 (1998).
[41] F.J. Femia, X. Chen, J.W. Babich, J. Zubieta. *Inorg. Chim. Acta*, **300–302**, 517 (2000).
[42] F. Mévelleca, A. Roucouxa, N. Noireta, H. Patina, L. Toupet. *Polyhedron*, **18**, 2537 (1999).
[43] F. Tisato, F. Refosco, M. Porchia, G. Bandoli, G. Pilloni, L. Uccelli, A. Boschi, A. Duatti. *J. Organomet. Chem.*, **637–639**, 772 (2001).
[44] K. Potgieter, P. Mayer, T.I.A. Gerber. *Aust. J. Chem.*, **63**, 1382 (2010).
[45] S. Chowdhury, A. Canlier, N. Koshino, Y. Ikeda. *Inorg. Chim. Acta*, **361**, 145 (2008).
[46] X. Chen, F.J. Femia, J.W. Babich, J. Zubieta. *Inorg. Chim. Acta*, **307**, 154 (2000).
[47] H. Spies, T. Fietz, H. Pietzsch, B. Johannsen, P. Leibnitz, G. Reck, D. Scheller, K. Klostermann. *J. Chem. Soc., Dalton Trans.*, 2277 (1995).
[48] H.J. Banberg, F.S. McQuillan, T.A. Hamor, C.J. Jones, J.A. McCleverty. *Inorg. Chim. Acta*, **170**, 23 (1990).
[49] W.A. Herrmann, M.U. Rauch, G.R.J. Artus. *Inorg. Chem.*, **35**, 1988 (1996).
[50] K.C. Potgieter, T.I.A. Gerber, P. Mayer. *S. Afr. J. Chem.*, **64**, 179 (2011).
[51] A.A. Danopoulos, A.C.C. Wong, G. Wilkinson, M.B. Hursthouse, B. Hussain. *J. Chem. Soc., Dalton Trans.*, 315 (1990).
[52] F. Refosco, F. Tisato, C. Bolzati, G. Bandoli. *J. Chem. Soc., Dalton Trans.*, 605 (1993).
[53] T.I.A. Gerber, D. Luzipo, P. Mayer. *J. Coord. Chem.*, **57**, 1345 (2004).
[54] J.P. O'Neil, S.R. Wilson, J.A. Katzenellenbogen. *Inorg. Chem.*, **33**, 319 (1994).
[55] L. Wei, J.W. Babich, J. Zubieta. *Inorg. Chem.*, **43**, 6445 (2004).
[56] C. Kremer, M. Rivero, E. Kremer, L. Suescun, A.W. Mombru, R. Mariezcurrena, S. Domnguez, A. Mederos, S. Midollini, A. Castineiras. *Inorg. Chim. Acta*, **294**, 47 (1999).
[57] R. Hübener, U. Abram, J. Strähle. *Acta Cryst.*, **C51**, 1284 (1995).
[58] B. Machura, M. Wolff, I. Gryca. *Polyhedron*, **30**, 142 (2011).

Downloaded by [Chongqing University] at 13:34 14 February 2014